Asif Jamil
Oh Pei Ching
Azmi B. M. Shariff

Department of Chemical Engineering, Universiti Teknologi PETRONAS, Bandar Seri Iskandar, Perak, Malaysia.

Current Status and Future Prospect of Polymer-Layered Silicate Mixed-Matrix Membranes for CO_2/CH_4 Separation

The mixed-matrix membrane (MMM), a state-of-the-art polymer-inorganic hybrid, is a relatively recent addition to the membrane family which adopts the synergistic advantages of the polymer and inorganic phase. Although marked improvement has been achieved by MMMs in CO_2/CH_4 separation, the development of a defect-free structure to transcend the Robeson upper bound limit remains a challenge. In previous years, a number of inorganic materials with diverse nature have been studied for CO_2/CH_4 separation; however, layered silicates have not attracted much attention despite their superior thermal and mechanical properties. Analyses of the potential of using layered silicates as inorganic fillers in MMM fabrication for CO_2/CH_4 separation are reviewed. Additionally, the immediate challenges toward successful formation of layered silicate-based MMM and future prospects are addressed.

Keywords: CO_2/CH_4 separation, Mixed-matrix membranes, Nanoclay, Polymer-layered silicate, Surface modification

Received: July 04, 2015; *revised:* December 30, 2015; *accepted:* March 08, 2016

DOI: 10.1002/ceat.201500395

1 Introduction

In recent years, gas separation via membrane technology has gained significant interest due to its versatility in processing, energy efficiency, low capital and operational cost, and small footprint [1, 2]. Nevertheless, polymeric membranes are limited by the trade-off trend (upper bound) between permeability and selectivity, as proposed by Robeson in 1991. Since data for predicting the initial upper bound curve was from permeability of various polymers but with limited emphases on membrane separation, the Robeson curve was later revised in 2008, thereupon provides an excellent comparison of the validity of upper bound concept and progress towards optimizing the structure/property relationship [3]. Fig. 1 depicts the past and present upper bound curve for polymeric and inorganic materials. According to this curve, inorganic materials show better separation properties as they exceed the upper bound whereas polymeric materials reside below the upper bound [4]. This reveals the superiority of inorganic materials over polymers in terms of selectivity. On the other hand, polymeric materials exhibit marginally higher permeability.

Separation membranes are classified based on differences in the transport mechanism, manufacturing materials or structural properties. For instance, mass transfer of gas through a membrane can involve several mechanisms such as solution diffusion, sorption diffusion, and molecular sieving. In terms of manufacturing materials, organic (polymer), inorganic or organic-inorganic hybrid materials are generally used for membrane fabrication. Similarly, membranes can be categorized according to their structural properties, namely porous, nonporous/dense, and asymmetric membranes [5].

Polymeric membranes are typically formed from either glassy or rubbery polymers. Rigid glassy polymers with small intersegment gaps, crystalline structures, and better chain interaction exhibit high intrinsic selectivity and low permeability. These glassy polymers generally have high chain entanglement and transport gas molecules on the basis of size and shape. Hence, small molecules easily pass through the voids between polymer chains whereas larger molecules are hindered by the rigid structure. In recent years, research efforts have focused on development of gas separation membranes based on rigid polymers due to their attractive mechanical and thermal properties as well as the aforementioned favorable characteristics [6, 7]. In contrast, rubbery polymers show the opposite behavior. They exhibit poor selectivity but relatively high permeability due to the lack of crystallinity, paucity of polar groups, and low degree of crosslinking. These rubbery polymers which consist of extremely flexible chains, permit gas molecules to pass through without obstruction, resulting in the high permeability but low selectivity. Several other parameters also affect membrane transport properties, i.e., polymer morphology, free volume content, chain segmental spacing, average molecular weight, glass transition temperature, and degree of crystallinity [2, 8].

Correspondence: Dr. Oh Pei Ching (peiching.oh@petronas.com.my), Department of Chemical Engineering, Universiti Teknologi PETRONAS, Bandar Seri Iskandar, 32610 Perak, Malaysia.

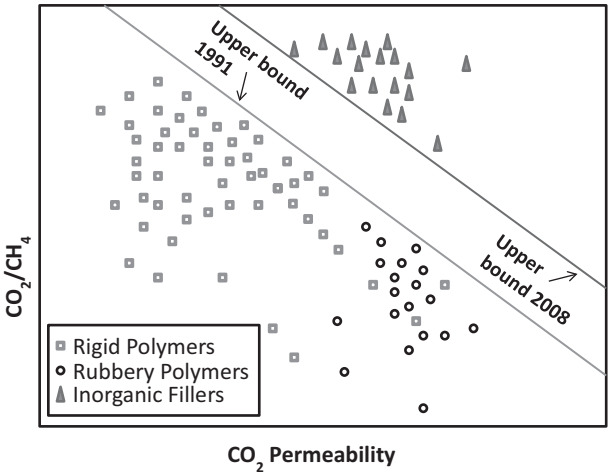

Figure 1. Robeson curve for CO_2/CH_4 gas pair permeability and selectivity.

For gas permeation, numerous polymers have been utilized to fabricate separation membranes. The most common include polyimide (PI), cellulose acetate (CA), polysulfone (PSf), polyethersulfone (PES), and polycarbonate (PC) [9–13]. In most cases, polymeric membranes are characterized by excellent processability, low cost, and demonstrate adequate separation performance at lower temperature and pressure. However, the efficiency often decreases in time due to chain compactness and thermal instability. Besides, swelling-induced plasticization generally occurs at higher gas pressure which ultimately reduces membrane permselectivity [14]. Inorganic membranes with molecular sieve-like properties show significantly higher diffusivity selectivity than polymeric membranes due to their discriminating ability based on pore sizes and shape. These membranes are also superior in terms of thermal and chemical stability, mechanical strength, and have a longer lifespan. Among the inorganic membranes, zeolite and carbon molecular sieve membranes favor CO_2/CH_4 separation due to narrow pore distribution. These membranes are able to withstand swelling induced by CO_2 gas at higher pressure and are stable at higher temperature. In spite of that, their commercial applications are hindered by the lack of technology to produce a defect-free membrane with improved reproducibility and at lower cost [15–17].

To overcome the limitations of polymeric and inorganic membranes, mixed-matrix membranes (MMMs) have emerged as one of the alternative approaches which afford enhanced gas separation performance. In this method, the superior gas separation properties, i.e., selectivity, of inorganic molecular sieve materials are combined with the desirable permeability, mechanical properties, and economical processability of polymers to fabricate a state-of-the-art hybrid membrane. In the early 1970s, Paul and Kemp started to embark on MMM research by incorporating 5Å zeolite in poly(dimethylsiloxane) (PDMS) to study the delayed diffusion time lag effect for CO_2 and CH_4 gas [18]. To date, Matrimid®, Udel®, and Ultem® are commercially available as viable polymers for incorporation of inorganic fillers in order to ameliorate gas separation properties [19–21]. Nonetheless, even though the usage of polymers with high glass transition temperature coupled with inorganic fillers is expected to produce MMMs which surpass the upper bound performance, poor combination of polymer/inorganic filler as well as poor adhesion at the polymer/inorganic filler interface, among others, caused deteriorated gas separation performance [22–24]. Hence, during selection of the appropriate inorganic filler to be incorporated into the organic phase, its shape, size, and interaction towards the penetrating molecules should also be considered for better membrane performance.

In this regard, it is found that inorganic particles with spherical shape minimize agglomeration whereas layered structures maximize polymer-filler contact. In addition, nano-sized fillers not only enhance polymer-filler interaction and assist in forming thin asymmetric MMMs, but also will interact with the penetrating molecules, resulting in increased permeation rate. Since the selection of an appropriate combination of polymer/inorganic filler is important in determining MMM performance, the next section will review the feasibility of using different inorganic sources, especially layered silicates as the filler [25].

2 MMM Interpenetrated with Organic Fillers

In essence, inorganic fillers are classified as porous or nonporous in nature. The mode of gas molecule transportation through a porous structure is diffusion mechanism whereas solubility selectivity is the transportation phenomenon for nonporous fillers. Inorganic fillers with porous structure include zeolite, carbon molecular sieves (CMSs), and carbon nanotubes (CNTs) whereas nanoclay, silica, and metal-organic frameworks (MOFs) represent nonporous structure [2, 26–29]. In literature, MMMs containing porous fillers, which are governed by diffusion as the dominating transport mechanism, have been extensively analyzed for CO_2/CH_4 application; however, less attention is paid for sorption selective systems.

In a polymer-layered silicate MMM, the mechanism for gas absorption and transportation is based on solubility. For the CO_2/CH_4 gas pair, due to lower critical temperature, CO_2 is more soluble compared to CH_4. Besides, the kinematic diameter for CO_2 is low which promotes faster diffusion. It is also interesting to note that polymers which contain polar groups such as ether oxygen, nitrile, and acetate, exhibit the highest CO_2 solubility selectivity. For example, when the ether oxygen concentration increases from polybutadiene to poly(tetramethylene) to poly(ethylene oxide), the CO_2 solubility also rises in the same order. In addition, the CO_2/CH_4 solubility selectivity of polymers also improves as the concentration of carbonyl and sulfone group increases [20, 30, 31].

Zeolite is one of the most widely used porous inorganic fillers incorporated in MMMs for CO_2/CH_4 separation. PSf/Matrimid® hollow-fiber membranes exhibited a 50 % increase in selectivity by adding zeolite to its selective skin layers [17, 32]. In comparison to neat polymers, addition of CMS to Matrimid® and Ultem® improved the membrane selectivity by 45 % and 40 %, respectively, for CO_2/CH_4 systems [25]. Much of this is due to the pore structure of porous fillers which provides discrimination of gas penetrants, thus enhances selectiv-

ity. Nonporous fillers, however, increase the free volume and dislocate chain packing, which lead to higher permeability. Poor adhesion with polymer matrix at the nanofiller surface might cause void formation that could result in higher permeability. By the addition of hydrated silica, i.e., nonporous inorganic filler, to polybenzimidazole (PBI), a solubility rise of condensable gases is reported in literature.

The presence of hydroxyl groups (–OH) in a polymer matrix plays a vital role towards solubility increase. Unlike the solution mechanism for gas transportation of hybrid membranes, in neat PBI membranes the diffusion permeation mechanism is responsible for gas transportation. Thus, reduced permeation of non-condensable gases is observed leading to gas separation in the presence of silica particles [33]. Nanoclay is another type of nonporous inorganic filler used extensively in the polymer composite industry, which exhibits good potential to be incorporated in MMMs for gas separation systems [34]. According to literature, very low clay loadings, i.e., $\leq$ 10 mass % clay, resulted in enhanced thermal, mechanical, optical, electrical, and barrier properties [35–40].

3 Layered Silicates

Layered silicates are naturally occurring or synthetically made minerals, and consist of very thin layers which are bonded to each other by counter-ions. The basic building block of layered silicates contains two core individual sheets, namely, a tetrahedral sheet in which silicon is surrounded by four oxygen atoms, and an octahedral sheet composed of aluminum encircled by eight oxygen atoms. Different combinations and arrangements of these tetrahedral and octahedral sheets form different kinds of molecular structure. For instance, in a 1:1 layered structure, a tetrahedral sheet is fused with an octahedral sheet and oxygen atoms are shared. In a 2:1 layered structure, an octahedral sheet is sandwiched between two tetrahedral sheets [41].

Fig. 2 shows the crystal lattice of 2:1 phyllosilicates. It consists of 2D layers where a central octahedral sheet of alumina is fused to two external silica tetrahedral sheets with shared apical oxygen atoms. Each layer is approximately 1 nm thick and lateral dimensions vary from 300 Å to several micrometers. The aspect ratio is usually greater than 1000 [42, 43]. Although layered silicates have achieved considerable commercial success as nanocomposites, their applications in MMMs are still in infancy stage and several fundamental issues like polymer-filler compatibility, dispersion etc. need to be addressed. Often, surface modification is performed to improve compatibility between layered silicates and the polymer matrix when synthesizing MMMs.

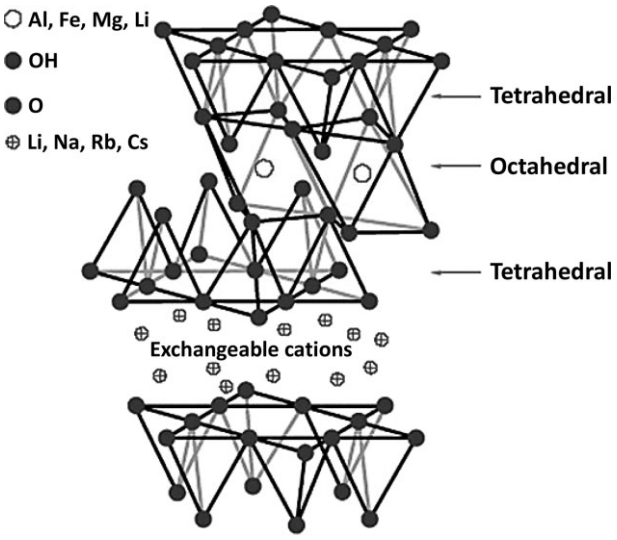

Figure 2. Structure of 2:1 phyllosilicate [49].

3.1 Clay Minerals

Clay minerals are layered silicates which belong to the phyllosilicate subclass and can be characterized based on their fine grained natural structure with sheet-like geometry. They exist in nature as tactoids with hundreds to thousands of silicate layers. Individual natural clay particles are generally smaller than 0.004 mm in diameter [44]. Clay minerals are further classified into subgroups such as smectite, illite, kaolinite, chlorite or sepiolite. Montmorillonite (MMT), a member of the smectite family, is extensively applied as reinforcing filler in the automotive industry since the 1990s. The Toyota Research group emerged as the pioneer in this regard, successfully commercializing nylon-6-MMT nanocomposite [45]. According to their findings, with a small addition of MMT (4.2 wt %), the modulus and tensile strength increased by 50 %. Since then, researchers have thoroughly investigated MMT application in thermoplastic nanocomposites due to their superior mechanical, barrier, thermal, flame-retardant, and abrasive properties [46–48].

The presence of charge in the tetrahedral and octahedral sheets influences the layered structure of clay minerals. The electronegative nature of the silicate layers attracts the exchangeable cations like Li^+, Na^+, Rb^+, and Cs^+ in the interlayer gallery spacing [34, 35]. The replacement of an element with another element in a mineral crystal without modifying its chemical structure is called isomorphous substitution and mainly results in charge development. For example, Al^{+3} can replace Si^{+4} in tetrahedral coordination, and replacement of Al^{+3} is possible by Mg^{+2}, Fe^{+2}, and Fe^{+3} in octahedral coordination [41]. In MMT, divalent Mg^{+2} replaces Al^{+3} and this creates surface charge disturbance which is balanced by Na^{+1} or Ca^{+2} ions. The interlayer spacing varies according to the size of the ions. Since these ions have an affinity for polar groups, water and other polar solvents can easily migrate inside the layer and cause it to expand [49]. This leads to high cationic exchange capacity of MMT, thus it is a promising inorganic filler for MMM development [50]. Tab. 1 summarizes the performance of clay as inorganic filler in MMMs for CO_2/CH_4 separation.

Along with MMT, bentonite, hectorite, saponite, and laponite are clays that are used as reinforcing fillers in polymer composite industry. Laponite is an entirely synthetic layered silicate that resembles the natural smectite mineral hectorite in both structure and composition. It is composed of six octahedral magnesium ions and two layers of four tetrahedral silicon atoms. The primary platelet size of laponite is only 25 nm

Table 1. Transport properties of layered silicates in different types of polymer matrix for CO_2/CH_4 separation applications.

Polymer	Nanofiller	Pressure [bar]	Temp. [°C]	Permeability Polymer (p)	Permeability MMM	Selectivity Polymer (α)	Selectivity MMM	Ref.
PEI	Cloisite15A (0.5 %)	15	25	0.63 barrers	0.78 barrers	79.6	101.89	[50]
PSf	Cloisite15A (1 %)	5	25	4.97 barrers	18.72 barrers	23.12	20.98	[34]
PEI	HNT (0.5 %)	15	25	0.63 barrers	0.80 barrers	79.6	85.97	[75]
PDMS	Sepiolite (20 %)	13.8	–	–	–	5.75	14.03	[67]
PDMS	TMA-MMT (15 %)	13.8	–	–	–	5.75	10.98	[67]
PBMA	Modified cloisite 15A (5 %)	4	25	56.3 barrers	24.6 barrers	9.4	10.25	[68]
PES	MMT-Na (2 %)	2	25	1.97 barrers	7.15 barrers	24.5	9.8	[76]
CA	AMH-3 (6 %)			7.55 barrers	11.59 barrers	29.61	29.71	[54]
PES	Cloisite 15A (0.25 %) coated with PDMS	3	25	2.70 barrers	9.77 barrers	28.38	33.49	[82]
PSF	C 5A (0.05 %)	5	25	19.88 GPU	5.48 GPU	23.12	14.81	[85]
PSF	C 15A (0.05 %)	5	25	19.88 GPU	4.53 GPU	23.12	52.67	[85]
PSF	C 30 B (0.05 %)	5	25	19.88 GPU	4.02 GPU	23.12	36.55	[85]

across by 1 nm thick, significantly smaller than its naturally occurring counterpart, because the synthetic laponite gel structures are formed under low-sheer-force systems in order to achieve homogeneity [51]. Similar to MMT, these clay fillers play an important role in the polymer nanocomposite industry due to their economic viability, availability, flame retardancy, and reinforcement characteristics. The interlayer space or "gallery", intercalation ability, and exfoliation of these layered clays enhanced their attractiveness as a component in polymer nanocomposites [46, 52].

3.2 Amherst-3

Amherst-3 (AMH-3) comprises a layered silicate structure with strontium cations, sodium cations, and water molecules between the layers. It has pores in 3D planes with 8-membered rings (8MRs) and pore size of 3.4 Å [53]. Fig. 3 depicts the AMH-3 structure, in which each layer is formed by bonding two silicate sheets containing 4MRs and 8MRs. AMH-3 possesses micropores in both parallel and perpendicular direction, promising state-of-the-art properties. In a recent study, AMH-3 is used to fabricate MMMs for gas separation applications to enhance permselectivity due to its unique 3D microstructure [54]. The microporosity of AMH-3 enhanced exfoliation in the polymer matrix, reduced permeation of larger gas molecules by creating a tortuous path, and as a result, high selectivity is achieved. Recently, it has been found that swelled AMH-3 with larger interlayer distance shows better properties than the intercalated phase. Nevertheless, the presence of silanol groups on the AMH-3 surface and the existence of charge-balancing cations between the intergallery spaces hinder AMH-3 swelling.

In a study, Choi introduced an innovative method, i.e., by sequential intercalation of dodecyl amine after proton exchange in the presence of amino acids, for the swelling of AMH-3 because the routine methods used for swelling of clays are not applicable for AMH-3 due to its strong interlayer bonding [55]. Also, conventional methods of dispersion and sonication do not guarantee exfoliation of AMH-3 in a polymer matrix. Hence, shear stress and viscosity of a polymer should be sufficiently high in order to achieve a high degree of exfoliation [56].

3.3 MCM-22

MCM-22 with a 2D aluminosilicate layered structure has found a variety of applications due to its versatile framework [57]. MCM-22 contains two independent porous systems, namely, a

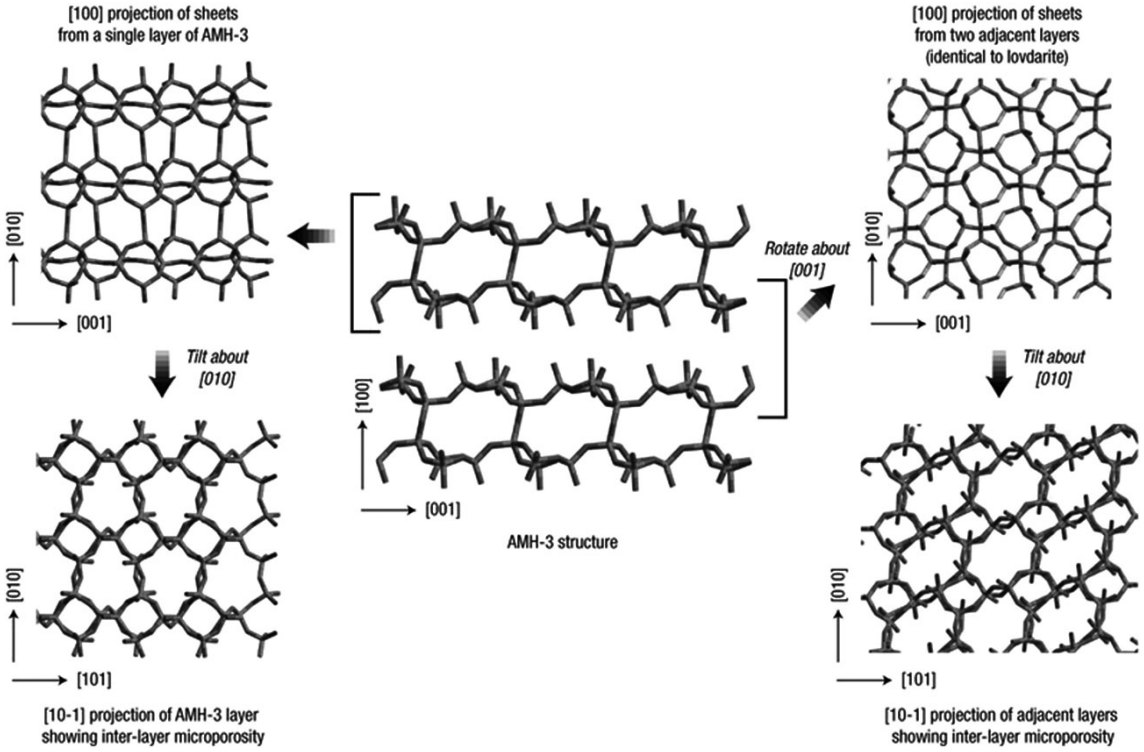

Figure 3. Projections of the AMH-3 structure. Top left: Projection of a single AMH-3 layer down [100]. Bottom left: Projection of the same layer along [101] showing 8MRs in the layer. Top right: Projection down [100] of two sheets from adjacent layers. Bottom right: Projection of the same down [10-1] showing an interlayer transport path through 8MRs. Red = Si, blue = O [53].

sinusoidal and bidirectional channel with internal diameter of 0.52 nm and other supercavities with 0.71 nm internal diameter. Both porous systems are accessible through 10MR windows [58]. Fig. 4 illustrates the schematic structure of MCM-22, highlighting the two independent porous systems. Kim et al. reported on functionalization of the layer surfaces of MCM-22 with hydrocarbon chain to increase hydrophobicity, as well as to perform interlayer swelling [59]. It is also found that amine-functionalized MCM-22 has promising features in CO_2 adsorption [60]. These characteristics evidence the potential of using MCM-22 as fillers in CO_2/CH_4 gas separation membranes [61].

Besides clay minerals, AMH-3 and MCM-22, several other synthetically modified layered silicates have been used, such as UZAR-S1, NU-6, and ITQ-2 [62–64].

4 Surface Modification of Layered Silicates

The hydrophilic nature of layered silicates makes them poorly suited to mixing and interacting with most polymer matrices. Moreover, the stacks of clay platelets are held together by electrostatic forces, whereby the counter-ions can be shared by two neighboring platelets, resulting in stacks of platelets that are held tightly together. Nanocomposites employing untreated clay would not exhibit much effectiveness, because most of the clay would form aggregates, involving very limited interaction between the matrix and the individual platelets.

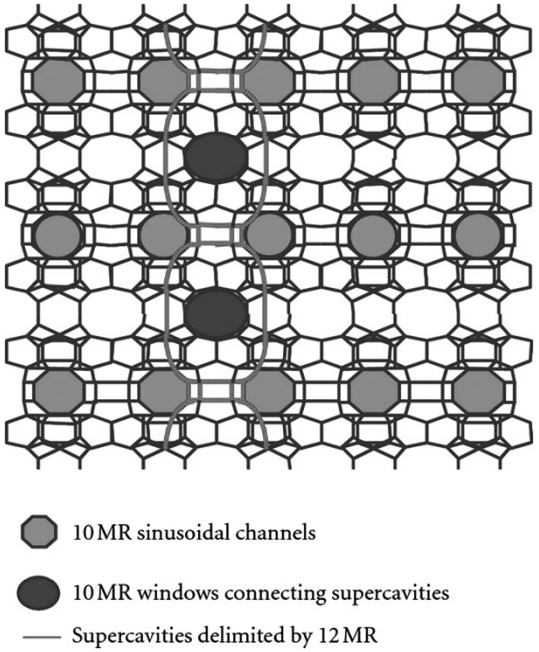

Figure 4. Graphical representation of MCM-22 [58].

A popular and relatively easy method of modifying the clay surface to render it more compatible with an organic matrix involves exchange of inorganic cations (Na^+ or Ca^{+2}). As can be

seen in Fig. 5, the inorganic cations are not strongly bound to the clay surface, thus, organic cations can replace them in the clay. For example, if sodium ions are replaced by quaternary ammonium ions (R_4N^+) with long alkyl chains, the clay would be more compatible with an organic matrix. This is due to the fact that the length of the alkyl chain imparts hydrophobicity in MMT. Therefore, by treating it with various organic cations, MMT clay can be compatibilized with a wide variety of matrix polymers [65].

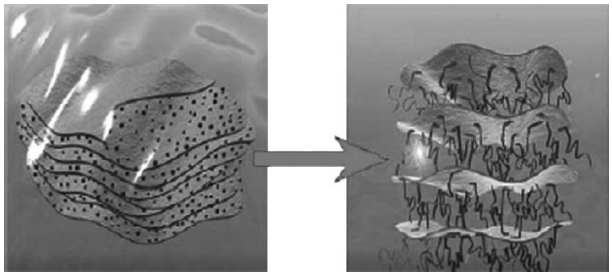

Figure 5. Schematic picture of ion exchange reaction. The relatively small inorganic ions (i.e., Na^{+1}) are exchanged by more voluminous organic onium cations [49].

Generally, two types of chemical modification, namely, noncovalent or covalent, can be performed on layered silicates. Noncovalent modification involves intercalation modification without covalent bonding through hydrogen bonding, Van der Waals interaction, dipole-dipole interactions, and acid base reactions. On the other hand, covalent bonding occurs through silylation, condensation, and esterification of SiOH/SiO_2 groups. The bonding forces involved in noncovalent modifications provide weaker interactions than covalent modifications, also organic cations provide functional groups that can interact or initiate polymerization of monomers to improve the strength of interface adhesion between the inorganic component and polymer phase. Thus, covalent modification not only increases the filler distribution but improves the MMM performance as well.

Fig. 6 summarizes the covalent and noncovalent modification of layered silicates with their possible applications [44, 66]. Defontaine et al. reported a considerable increase in membrane selectivity for CO_2/CH_4 by incorporating sepiolite and tetramethylammonium-intercalated montmorillonite (TMA-MMT) nanoclays in PDMS matrix [67]. A covalent bond was formed between the nanoclay surface and polymer chains by the silanol group. Addition of sepiolite nanofiller to the PDMS matrix resulted in an increase of 144 % in CO_2/CH_4 selectivity, due to the Si–O–Si bonding which occurred between the polymer chain and silicate layers due to the abundance of silanol groups present at the external surfaces. Whereas for TMA-MMT/PDMS MMMs, a 91 % increase in CO_2/CH_4 selectivity was achieved because of the lower density of edged silanol groups in MMT.

Along with the covalent and noncovalent approach, ion exchange is a relatively rapid method to achieve organophilicity of clay. For ion exchange, the interlayer ability to swell plays an important role. If alkali is present between the layers of clay, swelling is possible because divalent or trivalent atoms hinder the water molecules from penetrating the layers and inhibit the swelling process. The swelling flakes increase the selectivity for small molecules by creating a higher tortuous path for larger molecules. The common types of alkali cations used are sodium-based alkali cations such as octosilicate ($Na_8[Si_{32}O_{64}(OH)_8]\cdot 32H_2O$, also known as ilerite or RUB-18, α-$Na_2Si_2O_5$, and β-$Na_2Si_2O_5$, as well as non-sodium-based alkali cations such as $KHSi_2O_5$, $LiNaSi_2O_5\cdot 2H_2O$ (silinaite). The alkali cations present between the clay layers provide the opportunity for organic cations and surfactants to replace them.

Furthermore, the presence of interlayer organic cations decreases the surface energy, thus, interaction between polymer and modified clay improves significantly. The long-chained surfactants tethered at the surface of clay results in increased gallery space. This will attract polymer chains to diffuse into the gallery space and enhance interaction towards the polymer matrix. Ultimately, the compatibility of filler towards the polymer is also significantly improved [59]. Fig. 6 demonstrates the

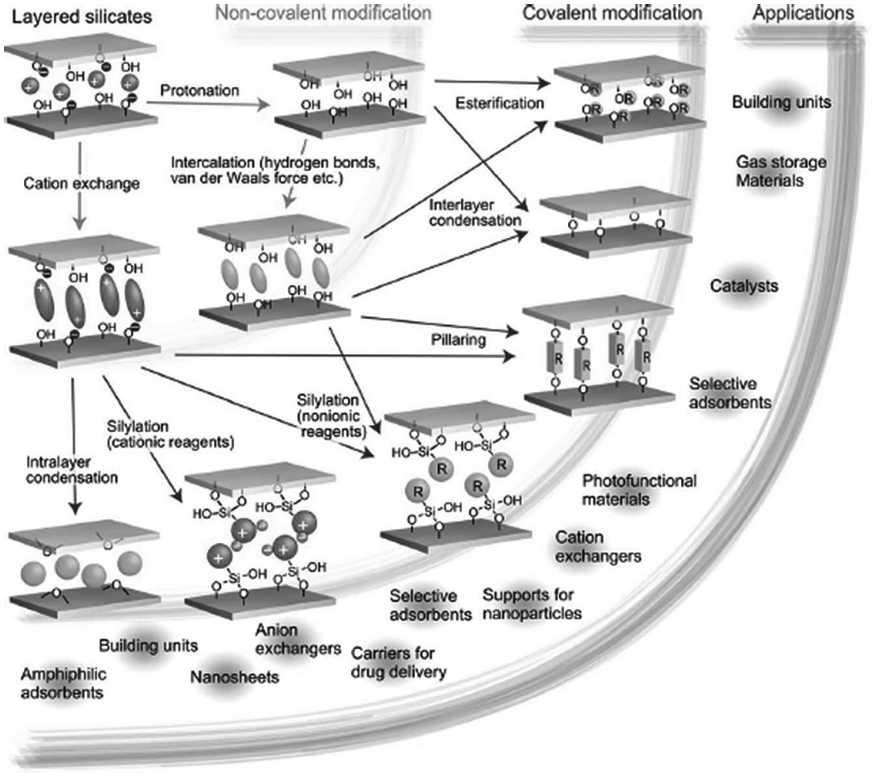

Figure 6. Types of modifications for layered silicates and their potential application areas [66].

ion exchange reaction of layered silicate, in which the Na^+ ion is replaced by the voluminous onium ion. After surface modification of layered silicate with surfactant molecules, the interlayer distance increased.

Alonso and co-workers modified naturally occurring MMT through ion exchange with [2-(acryloyloxy)ethyl]-trimethylammonium which creates tethered reactive groups on the surface of the silicate layer [68]. The modified MMT and poly(*n*-butylmethacrylate) are subsequently emulsion-polymerized to form a nanocomposite membrane. The tethered groups on the MMT surface were found to react with the acrylate monomers and exfoliate the silicate layers. Due to exfoliation, the tortuous path increases for the permeating gas, and, as a result, reduction in permeance is observed in spite of the increase in selectivity. This trend holds true for increasing filler loading. With 1 to 5 wt % filler loading, the selectivity increased by approximately 37 % whereas CO_2 permeability decreased by 31 % [69]. In another study, the authors used a similar modified MMT in poly(*n*-butylacrylate) to produce a nanocomposite membrane through in situ polymerization, which leads to exfoliated clay morphology within the polymer matrix. It was also found that with increasing modified MMT loading, the permeance reduction of CO_2 was approximately 56 % whereas 9.3 % enhancement in selectivity was achieved.

Cation-exchange capacity (CEC) represents the extent of negative charge on the surface of MMT and its ability to exchange ions. CEC is dependent on the isomorphous substitution in tetrahedral or octahedral layers of MMT. The CEC for MMT varies from 0.9 to 1.2 mequiv g^{-1} depending on the mineral origin. For nonpolar polymers, a quaternary alkyl having long alkyl chains is preferentially used whereas quaternary ammonium containing hydroxyl groups is considered to be suitable for polar polymer matrices [70]. Various types of MMT clay have been produced by changing the intercalated cations, each with its unique characteristic based on the interlayer distance. Tab. 2 summarizes some industrially available modified MMT clays and their interlayer distances.

5 Morphology of Polymer-Layered Silicate MMM

In fabricating enhanced-performance MMMs for gas separation, material selection remains the most crucial factor. In MMMs, the polymer phase improves permeation whereas dispersed fillers assist in raising the selectivity. When layered silicates are incorporated, three different types of morphological changes may take place, namely, dispersion, phase-separated and intercalated or exfoliated, as indicated in Fig. 7 [29]. These morphologies offer significant improvement in terms of mechanical, thermal, and barrier properties of polymer-nanoclay hybrid materials [34].

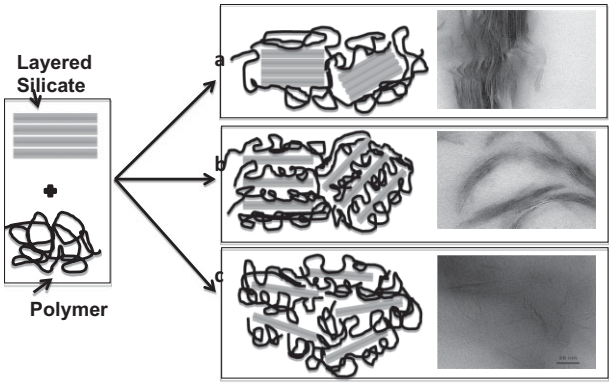

Figure 7. Schematic diagrams and TEM micrographs of layered silicates and polymer interfacial morphology. (a) Phase-separated, (b) intercalated morphology, (c) exfoliated morphology [43].

Principally, layered silicate affects the sorption of condensable gas by obstruction of diffusion pathways and reduction of the free volume in polymer systems [29, 71–73]. The exfoliated morphology creates a tortuous path for penetrating gas molecules. As a result, the permeance decreases at the expense of improved selectivity. Intercalation gives enhanced permeation but the risk of surface defects and void formation remains high for phase-separated and intercalated morphologies. Fig. 8

Table 2. Types of commercially available montmorillonite and their properties.

Filler	Clay type	Interlayer cations	Ammonium content [wt %]	Interlayer distance [Å]
Cloisite Na	Montmorillonite	Na^+	0	12.1
Cloisite 20A	Montmorillonite	$(CH_3)_2N^+$(hydrogenated tallow)$_2$	29.20	22.1
Cloisite 25A	Montmorillonite	$(CH_3)_2N^+$(hydrogenated tallow) (2-ethylhexyl)	26.90	20.7
Cloisite 30B	Montmorillonite	$(CH_3)_2N^+$(tallow)(CH_2CH_2OH)	20.30	18.5
Nanofil 757	Montmorillonite	Na^+	0	12.2
Nanofil 15	Montmorillonite	$(CH_3)_2N^+$(hydrogenated tallow)$_2$	28.90	29.0
Nanofil 919	Montmorillonite	$(CH_3)_2N^+$(tallow)$(CH_2C_6H_5)$	33.75	18.8
Nanofil 804	Montmorillonite	CH_3N^+(tallow)$(OH)_2$	30.08	18.0

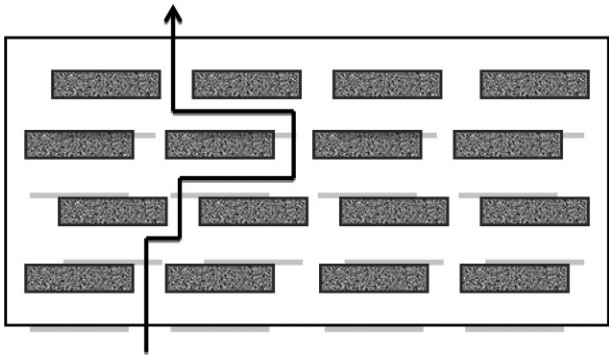

Figure 8. Schematic diagram of the tortuous path induced by the exfoliated structure in the polymer matrix.

shows the tortuous path induced by exfoliated clay layers in a polymer matrix.

The interface morphology between polymer and filler is also crucial in defect-free membrane development. The interface interaction actually decides the selective passage of one gas over the other, thus affecting the permeability and selectivity of gas molecules. Poor interaction leads towards nonideal morphologies as indicated in Fig. 9. These include sieve-in-a-cage, leaky interface, plugged interface, and chain rigidification. If polymer-filler adhesions are weak, interfacial voids will be formed at the polymer-filler interface, also known as sieve-in-a-cage morphology. These voids cause nonselective passage of the gas molecules, resulting in much higher permeability than the neat polymer, whereas selectivity may vary depending on the void size. When these interfacial voids become large enough so that gas molecules pass through without any resistance, the structure is known as leaky interface, which results in increased permeability but decreased selectivity. In chain rigidification, polymer chains are rigidified at the polymer-filler interface. This inhibits polymer chain mobilization at the interface, which lowers permeability as well as selectivity. Chain rigidification also causes pore blockage. Immobilized polymer chains may

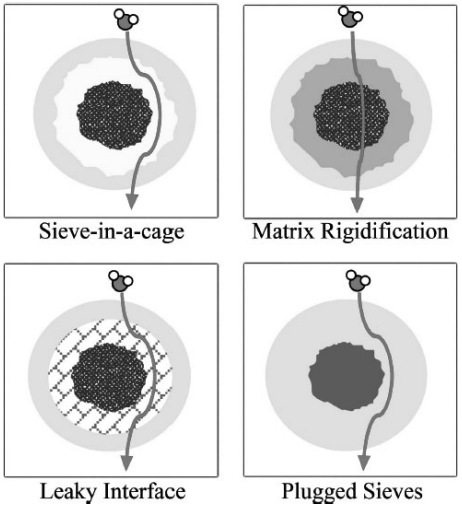

Figure 9. Nonideal polymer-filler morphology and transportation of gas [56].

block the pores of the filler, resulting in plugged fillers. All these defects in interface morphology seriously affect membrane performance. For this reason, various techniques are developed to reduce nonidealities in morphology such as priming protocol, selection of glassy polymers above T_g, grafting, use of silane coupling agents, and cross-linking techniques [29, 30, 56].

During membrane formation, the selection of solvent plays a vital role for membrane morphology. Whilst selecting the appropriate solvent, the interaction of solvent towards polymer and filler has to be carefully considered. There should be a strong polymer-filler interaction, fair polymer-solvent interaction, and weak filler-solvent interaction. If the polymer-solvent interaction is too strong, the polymer chains do not approach close to the filler surface. Conversely, if the filler-solvent interaction is too strong, it will be difficult for the solvent to desorb from the filler surface when the polymer chains approach the filler. Consequently, the order of interaction should be polymer/filler followed by polymer/solvent and filler/solvent [56].

6 Challenges and Issues in Successful Membrane Formation

6.1 Layered Silicate Dispersion in Organic Phase

The dispersion of nano-sized inorganic particles in the polymer matrix is the foremost challenge in MMM development. Generally, nanofillers disperse poorly in the polymer matrix, thus are likely to agglomerate in the MMM [74]. This tends to lead to the formation of numerous stress-concentrated points which can deteriorate the mechanical stability of MMM, especially at high inorganic filler concentrations. In order to promote dispersion, a surface priming protocol can be employed. In priming, a small amount of polymer is added to the nanofiller solution in order to decrease the interfacial stress between the polymer and nanofiller. This protocol is usually performed before the addition of bulk polymers to the nanofiller suspension.

Hashemifard demonstrated an interesting technique of modifying halloysite nanotubes (HNTs), a type of clay family, to improve the dispersion properties in the polymer matrix. In his work, the modification of HNT was performed with *N*-β-(aminoethyl)-γ-aminopropyltrimethoxysilane (AEAPTMS) and incorporated in the polyetherimide (PEI) matrix to analyze the adhesion and distribution [75]. Initially, the selectivity for HNT/PEI MMM decreased but the optimization of priming protocol and sonication extended the selectivity and dispersion of HNT platelets. His work also demonstrated that increased concentration of silane molecules leads to higher degree of tortuosity and ultimately higher selectivity. Moreover, the presence of an amine group in AEAPTMS/HNT/PEI MMM is also effectual in terms of CO_2 adsorption and improving CO_2 permeability and selectivity through the membrane. The optimum results achieved with 0.5 wt % of silylated HNT showed an increase of 28 % and 7 % in permeance and selectivity, respectively, as compared to a pristine PEI membrane.

6.2 Void Formation at the Filler Surface

Poor interaction of polymer chains and filler surface causes the formation of interfacial voids and results in poor membrane performance in terms of gas separation. To eliminate defects at the bulk polymer and dispersed filler interface, a priming protocol and silane coupling treatment have been proposed and reported in literature [17]. Silane coupling agents are effective in eliminating the interfacial voids by creating chemical linkages between the filler phase and organic matrix. They can react with hydroxyl groups, amino groups, and other functional groups from layered silicates and/or the polymer matrix to enhance the compatibility between the phase boundaries [17].

Hashemifard et al. reported a considerable increase in membrane selectivity for CO_2/CH_4 by incorporating raw and commercially modified MMT such as Cloisite 15A, in PEI matrix [50]. According to the study, Cloisite 15A provides better adhesion towards the PEI matrix due to the presence of dimethyl dehydrogenated tallow quaternary ammonium in the layered structure, which enhances MMM separation properties by minimizing void formation. Cloisite 15A not only improved adhesion due to the presence of a tallow interlayer gallery, its higher aspect ratio also favored the degree of tortuosity in the dense skin layer of MMM. As a result, a selectivity increase of 28 % is observed as compared to the pristine polymer as illustrated in Fig. 10. However, increasing the Cloisite 15A loading beyond the critical value resulted in agglomeration and void formation. The optimum membrane selectivity performance is observed at 0.5 % Cloisite 15A loading in the PEI matrix.

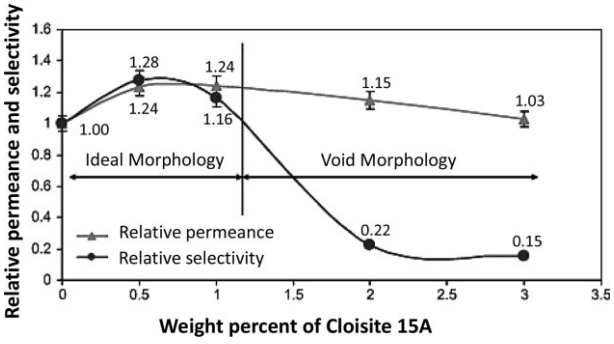

Figure 10. Effect of Cloisite 15A loading on PEI/Cloisite 15A MMM CO_2 permeance and CO_2/CH_4 selectivity [50].

Liang and co-workers also conducted a study on a polyethersulfone (PES)-based MMM with incorporation of Na-MMT as the inorganic filler [76]. The interlayer distance of MMT was found to grow with increasing filler loading, which suggested that polymer chains are intercalated in the gallery space. Nevertheless, at high filler loading, Na-MMT was found to agglomerate. This phenomena is evident as the permeability for CO_2 increased with Na-MMT loading but beyond 10 wt %, CO_2/CH_4 selectivity was greatly reduced. The authors speculate that the presence of interfacial voids leads to the decrease in membrane selectivity since gas transport occurs via Knudsen diffusion.

6.3 Distribution Morphology of Layered Silicates

The distribution of layered silicates in a polymer matrix is the most important parameter in order to control the membrane performance. Intercalated morphology leads to better permeation whereas exfoliated morphology favors selectivity by controlling the permeation of large-sized molecules. By using polysulfone (PSf) as polymer matrix and Cloisite 15A as filler, an asymmetric MMM was synthesized by Zulhairun which showed that at low Cloisite 15A loadings a 270 % enhancement in CO_2 permeability compared to neat PSf could be achieved without affecting CO_2/CH_4 selectivity [34]. The results were contrary to the concept that incorporation of clay filler caused permeability decrease. This may be largely dependent on how the clay minerals were dispersed in the polymer matrix, whether they were non-intercalated or phase-separated clay tactoids which might increase permeance. The authors have further speculated that unexfoliated clay layers may generate a high degree of perturbation in polymer chains packing, causing a higher permeance. Nanometer gaps around the inorganic phase causing possible Knudsen diffusion through clay galleries and polymer-clay interface might also affect permeability. By increasing the path length across MMM for large diffusion gases by capitalizing on the barrier properties of inorganic filler, the selectivity of small condensable gas could be enhanced among the gas mixture.

Nanocomposites of poly(ε-caprolactone) containing Na-MMT and Cloisite 30B were prepared by melt blending and in situ polymerization, and their gas barrier properties were analyzed by Gain and co-workers [77]. According to their study, along with the distribution of clay platelets in the polymer matrix, the processing technique and the interaction of polymer chains towards the clay surface are factors that influence the nanocomposite morphology. The intercalated spacing of Na-MMT and Cloisite 30B were 13.1 Å and 18.5 Å, respectively, in the polymer matrix.

Among others, melt processing and in situ polymerization are the most studied techniques to prepare polymer clay nanocomposites. Melt processing is an environmentally friendly technique without usage of a solvent whereas in situ intercalative polymerization involves the intercalation of a monomer in the gallery space of clay followed by polymerization. In situ polymerization leads to intercalated or exfoliated morphology which increases the platelet dispersion and delamination. The permeability of CO_2 decreases and it is found that the crystallinity of the polymer remains unchanged by the presence of nanoclay. The permeability reduction is higher for composites containing Cloisite 30B prepared through in situ polymerization despite their higher intergallery spacing. With the presence of hydroxyl functional groups, the grafting density increases, thus, less specific sites are available in the clay for gas sorption.

6.4 Polymer-Filler Compatibility

The compatibility of layered silicate towards the polymer matrix is another important aspect to be considered in MMM development. In order to increase polymer-filler compatibility, chemicals such as compatibilizers can be added to enhance the

interaction of the polymer matrix and layered silicates. The crystalline state is impermeable in nature; thus, reducing the crystallinity of a polymer phase leads to better permeability of penetrating gases. In previous research, highly crystalline high-density polyethylene (HDPE) and nanoclay (pristine and modified) nanocomposite films have been developed. It is observed that the crystallinity of HDPE is not affected by the addition of clay despite the permeability increase. This rise in permeability of HDPE/MMT-based nanocomposite membranes is due to the weak interaction between the polymer and filler interface. Therefore, addition of more polar maleic anhydride as compatibilizer increases intercalation, dispersion, exfoliation, and tortuous path, hence reduces permeability [70].

In recent literature, copolymer-layered silicate composite membranes are reported to be used for gas separation. Goodarzi prepared a polypropylene (PP)/ethyl vinyl acetate (EVA)/clay nanocomposite membrane to analyze the effect of morphology on gas permselectivity [78]. According to his research, EVA imparts better permeability properties in the polymer blend as compared to crystalline PP. The morphology and gas separation properties of the nanocomposite membrane have been investigated in the presence of organically modified montmorillonite (OMMT) and compatibilizers such as polypropylene grafted maleic anhydride (PP-g-MA). With the addition of OMMT, the carbonyl groups of EVA and hydroxyl group of OMMT results in intercalation. On the other hand, the presence of the compatibilizer helps increase the gallery space of OMMT and leads to exfoliated morphology. The higher the compatibilizer (PP-g-MA) content in the blend, the higher the distribution of OMMT in the composite. Addition of OMMT and compatibilizer to the PP/EVA blend causes lower gas permeability and higher selectivity due to the reduction in free volume fraction and increase in tortuous path. The CO_2 permeability in PP/EVA 75/25 blend decreases to 21.5 barrer when 5 wt % OMMT is added as compared to the blend without OMMT (25.6 barrer). Also, a further addition of 5 wt % compatibilizer reduced the permeability to 18.6 barrer.

Similar results were reported when organo (alkyl ammonium-modified) clay was added to a PP/ethylene-propylene-diene rubber (EPDM) blend by solvent blending technique. The irregularly shaped EPDM exists in the dispersed phase in the PP matrix with 50/50 composition blend. By the addition of organo clay, the dispersed phase transformed to almost spherical shape. An antioxidant generally known as Irgan is used as compatibilizer for better dispersion of nanoclay in the PP/EPDM blend.

The presence of a compatibilizer increases the gallery space of nanoclay. As a result, exfoliation morphology is obtained, thus, the tortuous path increases for diffusing molecules. Despite the decrease in crystallinity of PP, the permeability of CO_2 decreases with higher organo clay content [79]. The compatibilizers are used to improve the compatibility of polymer and nanoclay. It also changes the morphology of the polymer blend which results in a higher flake aspect ratio and exfoliated geometry that help in decreasing the permeation of CO_2 gas. On top of this, by increasing the tortuous path, selectivity is enhanced as well.

6.5 Polymer-Layered Silicates MMM Surface Defects

Since the surface structure of a membrane is crucial in enhancing membrane performance, extensive research has been carried out with regard to this aspect. Loeb and Sourirajan are the pioneers in developing integrally skinned asymmetric membranes in the 1960s [80]. An integrally skinned asymmetric membrane consists of two layers of the same materials. A very thin and dense skin layer (0.1–1 μm) is overlaid above a thick and highly porous sublayer (100–200 μm, void size 0.1–1 μm). The skin layer controls the diffusion and permeation of penetrating gases whereas the sublayer only provides mechanical support. High permeability can be achieved via the active thin skin layer, thus, any defect will cause poor gas separation performance [81].

Generally, surface defects in the thin skin layer can be minimized by controlling the casting shear rate, evaporation time, and by coating the membrane surface with a rubbery polymer. Ismail and co-workers prepared flat-sheet MMMs using PES and Cloisite 15A [82]. According to their findings, layered silicates bring about morphological changes in the polymer matrix and convert finger-like microvoids to sponge-like microvoids. At longer evaporation time, the skin layer obtained is thicker with aligned nanoparticles. As a result, the selectivity increase is significant as compared to lower evaporation time, due to the tortuous path near the surface. At 0.25 wt % Closite 15A loading, the permeability and selectivity decrease due to the development of the thin skin layer with nanoparticles coagulated near the surface. However, by prolonging the evaporation time, the membrane performance improved due to circulation and distribution in the skin layer. Besides, coating the membrane surface with PDMS improved the selectivity at the expense of permeability. The selectivity rise for coated membranes is approximately 227 % as compared to uncoated membranes at the same evaporation time.

On top of that, PVDF-hydrophilic MMT hollow-fiber MMMs are commonly used in gas liquid contactors. PVDF is hydrophobic in nature, thus, its concentration decreases during wet phase inversion near the outer surface resulting in a very thin skin layer. This is due to the fact that during membrane casting, tap water is used as external coagulant, nevertheless, the solvent and non-solvent do not diffuse out of the PVDF solution during phase inversion due to high hydrophobicity of PVDF. A decrease in dope viscosity with increment in solvent/coagulant exchange capacity is observed in the presence of MMT, due to the weaker polymer-clay interaction which reduces the thermodynamic stability of the polymer solution. A similar phenomenon is observed when adding sepiolite clay to chitosan and poly(vinyl alcohol) (PVA) as described by Huang et al. [83]. This reduction in polymer viscosity causes morphological changes and finger-like pores have been observed beneath the outer surface of the membrane. As a result, pores are generated in the thin skin layers, followed by a finger-like structure in the substrate which meets the sponge-like structure in the middle of the membrane. With increasing MMT loading, surface porosity and finger-like structure increases whereas the sponge-like zone gradually decreases which leads to perme-

ation enhancement. The maximum increment is observed at 5 wt % MMT loading where 21 % higher permeance is obtained compared to neat PVDF [84].

Another new approach which involves the incorporation of a selective flake that possesses lower thickness and higher aspect ratio leads to improved permeability without compromising the selectivity. Kim investigated the intercalation of primary amines in porous AMH-3 with cellulose acetate (CA) by using a high shear rate in order to obtain better exfoliation and higher aspect ratio [54]. The AMH-3 is also reacted with dodecylamine to induce swelling. The dodecylamine interlayer spacing is 30 Å whereas in AMH-3, the interlayer spacing decreased to 20 Å due to high normal forces induced by a high shear driving force mixer. Also, some of the dodecylamine molecules are extracted due to the shear force from the layers of AMH-3, leaving behind layers in close contact. The number of stacks of layer per tactoid is 3–8 for 2–6 % AMH-3. The CO_2/CH_4 gas separation performance of the AMH-3/cellulose acetate composite membrane is found to increase substantially with higher loading of flakes. The CO_2 permeability is increased by 54 % whereas selectivity remained very close to that of the pure CA matrix, i.e., 29.61. Thus, one envisages the future prospect of developing nano-flakes hybrid membranes which combine the advantages of high permeability while retaining the selectivity of the matrix.

Zulhairun also prepared MMMs by using a high aspect ratio of filler in order to avoid high filler loading that leads towards agglomeration, membrane surface defects, nonuniform morphology, and poor gas separation performance [85]. Closite 15A which is embedded in PSf is chemically modified with quaternary ammonium to render the hydrophilic surface hydrophobic along with a basal space increase to 3.46 Å. The initial dope solution is sonicated to disperse clay uniformly and a flat-sheet PSf-Closite 15A is fabricated. According to his findings, higher filler loading leads to diffusion path blockage and permeability reduction for gas molecules. By merely increasing 3 wt % of clay loading, the permeability of PSf-clay membrane is lowered by 80 %, and the optimum performance is observed at only 0.5 wt % filler loading.

The increase in clay loading leads to lower delamination or exfoliation of layers. As a result, a lower intergallery space is available for polymer molecules to intercalate, which contributes to lower distribution of clay within the polymer matrix. The number of stakes per tactoid reported to show optimal dispersion is 2–4. Excellent particle dispersion and interlayer void-free morphology is obtained, resulting in higher selectivity (by 144 %) for CO_2/CH_4 gases.

6.6 Plasticization

Plasticization is a phenomenon that takes place when the concentration of sorbing molecules increases to an extent that it swells the polymer matrix. Swelling typically occurs as a result of disturbance in chain mobility which ultimately reduces the separation ability of a membrane against the penetrating molecules. Generally, polymers having polar groups are more prone to plasticize because of the polarizing nature of the CO_2 molecule. For instance, $-OCOCH_3$ and $-COOCH_3$ are polar and flexible pendent groups in polymethyl methacrylate and polyethylmethacrylate (PEMA). These polymers are more likely to plasticize at higher CO_2 concentration [86]. In literature, several techniques have been proposed to address this issue, such as thermal treatment, polymer blending, and usage of cross-linking agents [87–91]. Thermal treatment suppresses membrane plasticization by densification of the polymer matrix and restricting the chain mobility. On the other hand, heat treatment decreases the free volume by improving the polymer chain packing [86]. In polymer blending, a polymer with high plasticization tendency is blended with another polymer which is stable against CO_2-induced plasticization. It has been reported that Matrimid® blended with PSf showed better plasticization resistance in mixed gas environment [92].

7 Conclusions and Future Prospects

In recent years, scientists are searching for robust new membrane materials to provide enhanced gas separation properties. Much work has been performed on polymeric membranes, nevertheless, their performance are not competitive at the industrial level. Inorganic membranes are too delicate to process and handle, however, they are capable to withstand higher pressure and temperature without reduction in separation ability. To date, polymeric membranes are still dominating the membrane gas separation market due to their ease of processing, despite their 5–10 times lower selectivity. To address this issue, mixed-matrix membranes (MMMs) are developed to fill the gap due to the inefficiency of polymeric and inorganic membranes.

In the past, various types of nanofillers, both porous and nonporous, have been studied for gas separation applications. Based on size and shape, porous fillers allow gas molecules to pass through whereas nonporous fillers are acknowledged to alter the chain orientation of polymers and improve the separation ability of the polymer matrix. Among the nonporous fillers, layered silicate exhibits the promising ability to alter polymer chain orientation. The selection of suitable polymeric material as matrix for layered silicate is essential for successful formation of membrane.

Similar techniques which are used to manufacture polymer membranes can be applied to fabricate MMMs. For instance, melt compounding which may produce direct exfoliation without using organic solvents, is an environmentally friendly, practical, and stable process that could be applied to fabricate MMMs dispersed with layered silicate [25]. Typically, the phase boundary defects between layered silicate and polymer phase results in poor membrane performance, nevertheless, these can be solved via crosslinking, thermal treatment, and priming protocol. The orientation of layered silicates is also a critical factor in defining the gas separation performance of MMMs, thus it should be carefully controlled during membrane casting.

Another interesting advantage of MMMs with layered fillers is that in most cases, the filler loading does not have to be very high to produce a significant permeation improvement. The development of high aspect ratio and nano-sized fillers open an interesting pathway to the production of asymmetric mixed-matrix hollow-fiber membranes with ultrathin selective

layers. The development of state-of-the-art ultrathin skinned layered MMMs could boost the performance of MMMs. For further advancement in this area, a high aspect ratio of layered silicates and a low number of stakes per tactoids should be ensured for low filler loading and enhanced dispersion.

The polymer-layered silicate interface void formation and distribution morphology are immediate challenges that have to be addressed. Along with improvement in existing materials, membrane researchers need to discover new materials to functionalize the layered silicate surfaces which may pave the way towards better dispersion and adhesion.

Acknowledgment

This work was supported by the Universiti Teknologi PETRONAS (UTP) and Ministry of Higher Education (MOHE), Malaysia, under URIF Grant No. 0153AA-B27 and MyRA Research Grant for CO_2 Rich Natural Gas Value Chain Program.

The authors have declared no conflict of interest.

References

[1] J. D. Figueroa, T. Fout, S. Plasynski et al., *Int. J. Greenhouse Gas Control* **2008**, *2 (1)*, 9–20. DOI: 10.1016/S1750-5836(07)00094-1
[2] T.-S. Chung et al., *Prog. Polym. Sci.* **2007**, *32 (4)*, 483–507. DOI: 10.1016/j.progpolymsci.2007.01.008
[3] L. M. Robeson, *J. Membr. Sci.* **2008**, *320 (1–2)*, 390–400. DOI: 10.1016/j.memsci.2008.04.030
[4] L. M. Robeson, *Curr. Opin. Solid State Mater. Sci.* **1999**, *4*, 549–552. DOI: 10.1016/S1359-0286(00)00014-0
[5] A. Jamil, O. P. Ching, A. B. M. Shariff, *Appl. Mech. Mater.: Trans. Tech. Publ.* **2014**, *625*, 690–695. DOI: 10.4028/AMM.625.690
[6] L. S. White, T. A. Blinka, H. A. Kloczewski, *J. Membr. Sci.* **1995**, *103 (1–2)*, 73–82. DOI: 10.1016/0376-7388(94)00313-N
[7] B. D. Freeman, *Macromolecules* **1999**, *32 (2)*, 375–380. DOI: 10.1021/ma9814548
[8] C. A. Scholes et al., *Int. J. Greenhouse Gas Control* **2010**, *4 (5)*, 739–755. DOI: 10.1016/j.ijggc.2010.04.001
[9] S. C. Pesek, W. J. Koros, *J. Membr. Sci.* **1993**, *81*, 71–88. DOI: 10.1016/0376-7388(93)85032-R
[10] J. D. Wind, D. R. Paul, W. J. Koros, *J. Membr. Sci.* **2004**, *228 (2)*, 227–236. DOI: 10.1016/j.memsci.2003.10.011
[11] A. Y. Houde et al., *J. Appl. Polym. Sci.* **1996**, *62 (13)*, 2181–2192.
[12] H. Kumazawa, J. S. Wang, E. Sada, *J. Polym. Sci., Part B: Polym. Phys.* **1993**, *31 (7)*, 881–886. DOI: 10.1002/polb.1993.090310716
[13] S. Sridhar, T. M. Aminabhavi, M. Ramakrishna, *J. Appl. Polym. Sci.* **2007**, *105 (4)*, 1749–1756. DOI: 10.1002/app.24628
[14] Z. Y. Yeo, T. L. Chew, P. W. Zhu, *J. Nat. Gas Chem.* **2012**, *21 (3)*, 282–298. DOI: 10.1016/S1003-9953(11)60366-6
[15] R. Nasir et al., *Chem. Eng. Technol.* **2013**, *36 (5)*, 717–727. DOI: 10.1002/ceat.201200734
[16] M. Muhammad et al., *Sep. Purif. Rev.* **2014**, *44 (4)*, 331–340. DOI: 10.1080/15422119.2014.970195
[17] Y. Zhang et al., *Int. J. Greenhouse Gas Control* **2013**, *12*, 84–107. DOI: 10.1016/j.ijggc.2012.10.009
[18] D. R. Paul, D. R. Kemp, *J. Polym. Sci.: Polym. Symp.* **1973**, *41 (1)*, 79–93. DOI: 10.1002/polc.5070410109
[19] C. M. Zimmerman, A. Singh, W. J. Koros, *J. Membr. Sci.* **1997**, *137*, 145–154. DOI: 10.1016/S0376-7388(97)00194-4
[20] H. Lin, B. D. Freeman, *J. Mol. Struct.* **2005**, *739 (1–3)*, 57–74. DOI: 10.1016/j.molstruc.2004.07.045
[21] D. Q. Vu, W. J. Koros, S. J. Miller, *J. Membr. Sci.* **2003**, *211 (2)*, 311–334. DOI: 10.1016/S0376-7388(02)00429-5
[22] J. M. Duval et al., *J. Appl. Polym. Sci.* **1994**, *54*, 409–418.
[23] R. Mahajan et al., *J. Appl. Polym. Sci.* **2002**, *86 (4)*, 881–890. DOI: 10.1002/app.10998
[24] R. Mahajan, W. J. Koros, *Ind. Eng. Chem. Res.* **2002**, *39*, 2692–2696.
[25] C. Rubio, B. Zornoza et al., *Curr. Org. Chem.* **2014**, *18*, 2351–2363.
[26] Y. K. Kim, H. B. Park, Y. M. Lee, *J. Membr. Sci.* **2005**, *255*, 265–273. DOI: 10.1016/j.memsci.2005.02.002
[27] M. Sadeghi et al., *J. Membr. Sci.* **2011**, *376 (1–2)*, 188–195. DOI: 10.1016/j.memsci.2011.04.021
[28] M. Schwanninger et al., *Vib. Spectrosc.* **2004**, *36 (1)*, 23–40. DOI: 10.1016/j.vibspec.2004.02.003
[29] P. S. Goh et al., *Sep. Purif. Technol.* **2011**, *81 (3)*, 243–264. DOI: 10.1016/j.seppur.2011.07.042
[30] A. L. Khan, C. Klaysom, C. A. Gahlaut et al., *J. Membr. Sci.* **2013**, *447*, 73–79. DOI: 10.1016/j.memsci.2013.07.011
[31] D. Bera et al., *J. Membr. Sci.* **2014**, *453*, 175–191. DOI: 10.1016/j.memsci.2013.10.073
[32] D. Q. Vu, W. J. Koros, S. J. Miller, *Ind. Eng. Chem. Res.* **2003**, *42*, 1064–1075. DOI: 10.1016/S0376-7388(03)00245-X
[33] M. Sadeghi, M. A. Semsarzadeh, H. Moadel., *J. Membr. Sci.* **2009**, *331 (1–2)*, 21–30. DOI: 10.1016/j.memsci.2008.12.073
[34] A. K. Zulhairun et al., *Chem. Eng. J.* **2014**, *241*, 495–503. DOI: 10.1016/j.cej.2013.10.042
[35] Y. W. Chen-Yang et al., *Polymer* **2007**, *48 (10)*, 2969–2979. DOI: 10.1016/j.polymer.2007.03.024
[36] X. Fu, S. Qutubuddin, *Polymer* **2001**, *42 (2)*, 807–813. DOI: 10.1016/S0032-3861(00)00385-2
[37] T. G. Gopakumar et al., *Polymer* **2002**, *43 (20)*, 5483–5491. DOI: 10.1016/S0032-3861(02)00403-2
[38] H.-L. Tyan, Y.-C. Liu, K.-H. Wei, *Chem. Mater.* **1999**, *11 (7)*, 1942–1947. DOI: 10.1021/cm990187x
[39] J. W. Gilman et al., *Chem. Mater.* **2000**, *12 (7)*, 1866–1873. DOI: 10.1021/cm0001760
[40] K. Prashantha et al., *Int. J. Polym. Anal. Charact.* **2014**, *19*, 363–371. DOI: 10.1080/1023666X.2014.902715
[41] F. Uddin, *Metall. Mater. Trans. A* **2008**, *39*, 2804–2814. DOI: 10.1007/s11661-008-9603-5
[42] P. Anadao et al., *J. Membr. Sci.* **2014**, *455*, 187–199. DOI: 10.1016/j.memsci.2013.12.081
[43] V. Mittal, *Materials* **2009**, *2*, 992–1057.
[44] F. Z. Annabi-Bergaya, *Microporous Mesoporous Mater.* **2008**, *107 (1–2)*, 141–148. DOI: 10.1016/j.micromeso.2007.05.064
[45] Q. T. Nguyen, D. G. Baird, *Adv. Polym. Tech.* **2006**, *25*, 270–285. DOI: 10.1002/adv.20079
[46] A. Okada, A. Usuki, *Mater. Sci. Eng., C* **1995**, *3*, 109–115. DOI: 10.1016/0928-4931(95)00110-7

[47] A. Usuki et al., *J. Appl. Polym. Sci.* **1995**, *55*, 119–123. DOI: 10.1002/app.1995.070550113

[48] Y. Kojima et al., *J. Polym. Sci., Part B: Polym. Phys.* **1995**, *33*, 1039–1045. DOI: 10.1002/polb.1995.090330707

[49] S. Pavlidou, C. D. Papaspyrides, *Prog. Polym. Sci.* **2008**, *33*, 1119–1198. DOI: 10.1016/j.progpolymsci.2008.07.008

[50] S. A. Hashemifard, A. F. Ismail, T. Matsuura, *Chem. Eng. J.* **2011**, *170*, 316–325. DOI: 10.1016/j.cej.2011.03.063

[51] A. M. Herring, *J. Macromol. Sci., Polym. Rev.* **2006**, *46*, 245–296. DOI: 10.1080/00222340600796322

[52] S. J. Ahmadi, Y. D. Huang, W. Li, *J. Mater. Sci.* **2004**, *39*, 1919–1925. DOI: 10.1023/B:JMSC.0000017753.90222.96

[53] H.-K. Jeong et al., *Nat. Mater.* **2003**, *2*, 53–58. DOI: 10.1038/nmat795

[54] W.-G. Kim et al., *J. Membr. Sci.* **2013**, *441*, 129–136. DOI: 10.1016/j.memsci.2013.03.044

[55] S. Choi et al., *Microporous Mesoporous Mater.* **2008**, *115 (1–2)*, 75–84. DOI: 10.1016/j.micromeso.2007.12.041

[56] M. Rezakazemi et al., *Prog. Polym. Sci.* **2014**, *39 (5)*, 817–861. DOI: 10.1016/j.progpolymsci.2014.01.003

[57] M. E. Leonowicz, J. A. Lawton et al., *Science* **1994**, *264*, 1910–1913. DOI: 10.1126/science.264.5167.1910

[58] U. Diaz, *ISRN Chem. Eng.* **2012**, Article ID 537164. DOI: 10.5402/2012/537164

[59] W.-G. Kim, S. Choi, S. Nair, *Langmuir* **2011**, *27 (12)*, 7892–7901. DOI: 10.1021/la200851j

[60] S.-T. Yang et al., *Fuel* **2014**, *974*, 35–442.

[61] J. Choi, M. Tsapatsis, *J. Am. Chem. Soc.* **2010**, *132 (2)*, 448–449. DOI: 10.1021/ja908864g

[62] S. Choi et al., *J. Membr. Sci.* **2008**, *316 (1–2)*, 145–152. DOI: 10.1016/j.memsci.2007.09.026

[63] A. Galve et al., *J. Membr. Sci.* **2011**, *370 (1–2)*, 131–140. DOI: 10.1016/j.memsci.2011.01.011

[64] P. Gorgojo et al., *Microporous Mesoporous Mater.* **2011**, *142*, 122–129. DOI: 10.1016/j.micromeso.2010.11.025

[65] N. Nassar, L. A. Utracki, M. R. Kamal, *Int. Polym. Process.* **2005**, *20 (4)*, 423–431.

[66] N. Takahashi, K. Kuroda, *J. Mater. Chem.* **2011**, *21*, 14336–14353. DOI: 10.1039/C1JM10460H

[67] G. Defontaine et al., *J. Colloid Interface Sci.* **2010**, *343 (2)*, 622–627. DOI: 10.1016/j.jcis.2009.11.048

[68] J. M. Herrera-Alonso, Z. Sedlakova, E. Marand, *J. Membr. Sci.* **2010**, *349 (1–2)*, 251–257. DOI: 10.1016/j.memsci.2009.11.057

[69] J. M. Herrera-Alonso, Z. Sedlkov, E. Marand, *J. Membr. Sci.* **2010**, *363 (1–2)*, 48–56. DOI: 10.1016/j.memsci.2010.07.014

[70] E. Picard et al., *J. Colloid Interface Sci.* **2007**, *307 (2)*, 364–376. DOI: 10.1016/j.jcis.2006.12.006

[71] C. Silvestre, D. Duraccio, S. Cimmino, *Prog. Polym. Sci.* **2011**, *36 (12)*, 1766–1782. DOI: 10.1016/j.progpolymsci.2011.02.003

[72] J. P. G. Villaluenga et al., *Eur. Polym. J.* **2007**, *43 (4)*, 1132–1143. DOI: 10.1016/j.eurpolymj.2007.01.018

[73] H. Monteiro Cordeiro De Azeredo, *Food Res. Int.* **2009**, *42*, 1240–1253. DOI: 10.1016/j.foodres.2009.03.019

[74] P. C. Oh, N. A. Mansur, *Jurnal Teknologi* **2014**, *69*.

[75] S. A. Hashemifard, A. F. Ismail, T. Matsuura, *J. Colloid Interface Sci.* **2011**, *359 (2)*, 359–370. DOI: 10.1016/j.jcis.2011.03.077

[76] C.-Y. Liang et al., *Sep. Purif. Technol.* **2012**, *92*, 57–63. DOI: 10.1016/j.seppur.2012.03.016

[77] O. Gain et al., *J. Polym. Sci., Part B: Polym. Phys.* **2005**, *43*, 205–214. DOI: 10.1002/polb.20316

[78] V. Goodarzi et al., *Polym. Degrad. Stab.* **2010**, *95 (5)*, 859–869. DOI: 10.1016/j.polymdegradstab.2010.01.009

[79] M. Frounchi et al., *J. Membr. Sci.* **2006**, *282 (1–2)*, 142–148. DOI: 10.1016/j.memsci.2006.05.016

[80] S. Loeb, S. Sourirajan, *Saline Water Convers. II* **1963**, 117–132.

[81] A. F. Ismail, P. Y. Lai, *Sep. Purif. Technol.* **2004**, *40*, 191–207. DOI: 10.1016/j.seppur.2004.02.011

[82] N. M. Ismail, A. F. Ismail, A. Mustaffa, *Jurnal Teknologi* **2014**, *69 (9)*, 83–87.

[83] D. Huang, B. Mu, A. Wang, *Mater. Lett.* **2012**, *86*, 69–72. DOI: 10.1016/j.matlet.2012.07.020

[84] M. Rezaei et al., *Chem. Eng. Res. Des.* **2014**, *92 (11)*, 2449–2460. DOI: 10.1016/j.cherd.2014.02.019

[85] A. K. Zulhairun, A. F. Ismail, *J. Membr. Sci.* **2014**, *468*, 20–30. DOI: 10.1016/j.memsci.2014.05.038

[86] A. F. Ismail, W. Lorna, *Sep. Purif. Technol.* **2002**, *27 (3)*, 173–194. DOI: 10.1016/S1383-5866(01)00211-8

[87] S. Shahid, K. Nijmeijer, *J. Membr. Sci.* **2014**, *470*, 166–177. DOI: 10.1016/j.memsci.2014.07.034

[88] A. F. Ismail, W. Lorna, *Sep. Purif. Technol.* **2003**, *30*, 37–46. DOI: 10.1016/S1383-5866(02)00097-7

[89] J. D. Wind et al., *Macromolecules* **2003**, *36 (6)*, 1882–1888. DOI: 10.1021/ma025938m

[90] C. Cao, T. S. Chung, Y. Liy et al., *J. Membr. Sci.* **2003**, *216*, 257–268. DOI: 10.1016/S0376-7388(03)00080-2

[91] D. Sen, H. Kalipcilar, L. Yilmaz, *J. Membr. Sci.* **2007**, *303 (1–2)*, 194–203. DOI: 10.1016/j.memsci.2007.07.010

[92] A. Bos et al., *AIChE J.* **2001**, *47*, 1088–1093. DOI: 10.1002/aic.690470515

Review: Mixed-matrix membranes (MMMs) were developed to overcome the limitations of polymeric and inorganic membranes and are regarded as state-of-the-art polymer-inorganic hybrids. Potential applications of layered silicates as inorganic fillers in MMM fabrication for CO_2/CH_4 separation are reviewed together with challenges for successful formation of layered silicate-based MMMs and future prospects.

Current Status and Future Prospect of Polymer-Layered Silicate Mixed-Matrix Membranes for CO_2/CH_4 Separation

A. Jamil, O. P. Ching*, A. B. M. Shariff

Chem. Eng. Technol. **2016**, *39 (XX)*, XXX … XXX

DOI: 10.1002/ceat.201500395